EARLY AGE THERMAL AND SHRINKAGE CRACKS IN CONCRETE STRUCTURES – INFLUENCE OF GEOMETRY AND DIMENSIONS OF A STRUCTURE

Barbara KLEMCZAK [a], Agnieszka KNOPPIK-WRÓBEL [b]

[a] DSc; Faculty of Civil Engineering, Silesian University of Technology, Akademicka 5, 44-100 Gliwice, Poland
E-mail address: *barbara.klemczak@polsl.pl*

[b] MSc; Faculty of Civil Engineering, Silesian University of Technology, Akademicka 5, 44-100 Gliwice, Poland
E-mail address: *agnieszka@knoppik.pl*

Abstract

The issues related to early age cracking of concrete structures are discussed in the paper. The main cause of these cracks are inhomogeneous volume changes associated with thermal and moisture gradients occurring in structures due to the hydration process. The paper discusses the influence of the type and dimensions of a structure on the distribution of temperature, moisture and induced stresses. Two types of structures with different dimensions are analyzed: the massive foundation slab as the example of internally restraint structure and the reinforced concrete wall as the example of externally restraint structure.

Streszczenie

Zagadnienia prezentowane w artykule są związane z wczesnymi rysami powstającymi w konstrukcjach betonowych. Główną przyczyną powstawania tych rys są nierównomierne zmiany objętościowe twardniejącego betonu związane z powstającymi w procesie twardnienia betonu gradientami temperatur i wilgotności. W artykule analizowano wpływ typu i wymiarów konstrukcji na rozkład temperatur twardnienia betonu, zmian wilgotności i generowanych naprężeń. Analizowano dwa typy konstrukcji: masywne płyty fundamentowe jako przykład konstrukcji z więzami wewnętrznymi oraz ściany żelbetowe będące przykładem konstrukcji z więzami zewnętrznymi.

1. INTRODUCTION

The hydration of cement is a highly exothermal reaction and as a result concrete elements are subjected to temperature variations. In structural elements with thin sections the generated heat dissipates quickly and causes no problem. In thicker sections the internal temperature can reach a significant level. Furthermore, the internal temperature drops slowly while the surfaces with direct contact with environment cool rapidly. As a result, thermal gradients occur across the section of concrete elements. There are also moisture gradients due to the differences in loss of moisture from the surfaces and from the core of the element.

The volume changes due to the temperature and moisture variation have consequences in arising stresses in a concrete element. These stresses can be defined as self-induced stresses – they are related to internal restraints of the structure, resulting from non-uniform volume changes in a cross section. In internally restraint elements during the phase of temperature increase tensile stresses originate in surface layers of the element and compressive stresses are observed inside the element. An inversion of the stress body occurs during the cooling phase: inside we observe tensile stresses, in the surface layers – compressive stresses. The self-induced stresses can be expected, for

example, within thick foundation slabs, thick walls, dams and each element with interior temperatures considerably greater than surface temperatures. In such elements, usually described as massive structures, random crack maps on surfaces can be usually observed.

The crucial question here is: what elements are sensitive to the early age thermal and shrinkage effects and when they can be classified as a massive structure. In ACI 116R massive concrete is defined as "any volume of concrete with dimensions large enough to require that measures to be taken to cope with the generation of heat and attendant volume change to minimize cracking" [1]. Because it is not the precise definition, some measures are proposed to estimate the early age thermal cracking tendency. One of them, proposed by Flaga [2, 3, 4], is related to the surface modulus defined as:

$$m = \frac{S}{V} \qquad (1)$$

where S is the area of surfaces and V is the volume of element.

According to the above mentioned proposal given by Flaga, the concrete element is defined as mass or thick element that is sensitive to early age thermal effects when $m < 2$. In such elements the expected increase of temperature is greater than 20°C. When $2 \leq m \leq 15$ the element is defined as medium-thick and the expected increase of temperature is lower than 20°C. It should be also mentioned that in medium-thick elements the shrinkage effects play more important role than in mass elements.

Coefficient m takes into account only the geometry of the structure. Therefore, in case when only a part of surfaces is cooled, more relevant measure of thermal cracking sensitivity is the apparent surface modulus [5] defined as:

$$m_p = \frac{S_p}{V} \qquad (2)$$

where S_p is the area of surfaces which is cooled.

Another proposed measure for concrete elements is an equivalent thickness [5, 6] defined as:

$$d_e = \frac{V}{S_p} \qquad (3)$$

Additionally, the concrete element can be externally restrained. For example, such a restraint exists along the contact surface of mature concrete against which

the new concrete element has been cast. In such case the forced stresses related to limitation of structure deformations freedom are also induced. The forced stresses are often observed in medium- thick elements such as wall cast against an old set concrete. In this case a series of vertical cracks starting from the base are usually observed [7]. It should be also pointed that the stresses resulting from external restrain of structure add to the effects of internal restraint. However, if high external restraint conditions exist, the effects of internal restraint are negligible.

The paper discusses the influence of the type and dimensions of a structure on the distribution of temperature, moisture and induced stresses. Two types of structures with different dimensions are analyzed for assumed material, environmental and technological conditions. One of them is the massive foundation slab as an example of internally restraint structure. The second one is a reinforced concrete wall as an example of externally restraint structure. Presented numerical results that illustrate the discussed problem were obtained with the programs TEMWIL, MAFEM_VEVP and MAFEM3D. The numerical model applied in the above mentioned programs can be classified as a phenomenological model. The influence of the mechanical fields on the temperature and moisture fields was neglected, but the thermal-moisture fields were modeled using the coupled equation of the thermodiffusion. Therefore, complex analysis of a structure consists of three steps. The first step is related to determination of temperature and moisture development, in the second one thermal-shrinkage strains are calculated and these results are used as an input for computation of stress in the last step. For the purpose of determination of the stress state in the early-age concrete structures the viscoelasto-viscoplastic model with a consistent conception was proposed. Full description of the model and computer programs: TEMWIL, MAFEM_VEVP and MAFEM3D, is contained in [8, 9].

2. MASSIVE FOUNDATION SLABS

The object of the conducted analyses was the massive foundation slab with different base dimensions: 5 m × 5 m, 10 m × 10 m, 20 m × 20 m and different thicknesses: 1m, 2m, 3m. It was assumed that the analyzed slab was made of the following concrete mix: cement CEM II/BS 32.5R 350 kg/m³, water 175 l/m³, aggregate 1814 kg/m³. The foundations were assumed to be reinforced with a 20 cm × 20 cm mesh at the top, bottom and side surfaces. Steel class RB400 and

ϕ12 bars were assumed for calculations. The finite element mesh of the analyzed slab has been shown in Figure 1. Because of the symmetry only the quarter of the slab is modeled. Essential elements of the slab that were used in presentation of calculation results have been marked with black color in Figure 1.
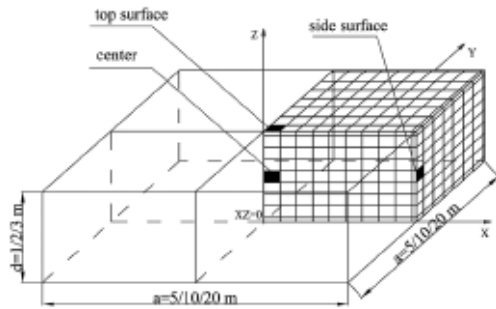
Figure 1.
Dimensions of massive foundation slab with the assumed finite element mesh

The development of mechanical properties in time was assumed according to CEB-FIP MC90 [7]. The final values for 28-day concrete were assumed as following: the compressive strength f_{cm} = 32.4 MPa, the tensile strength f_{ctm} = 3.0 MPa and the modulus of elasticity E_{cm} = 32 GPa. Environmental and technological conditions were taken as: ambient temperature 20°C, initial temperature of fresh concrete mixture 20°C, wooden formwork of 1.8 mm plywood on bottom and side surfaces; no insulation and no protection of top surface. It was also assumed that formwork is removed in 28 days after concrete casting. Thermal and moisture coefficients necessary for calculations have been set in Table 1.

Firstly, the temperature and moisture development were analyzed in slabs with different dimensions. The results are shown in Figure 2a, Figure 2c, Figure 2e, Figure3a and Figure 3b. It can be noticed that the character of temperature development and values of temperatures generated during the curing process does not depend on the base dimensions of the slab. It is also perfectly visible that the thickness of the slab has the main influence on the temperature development and values of generated temperatures. The greatest temperature, equal to 54.4°C, is reached in the center of the thickest slab (d = 3m) after 5.1 days of concrete curing. In slabs with smaller thickness maximum temperatures occurred earlier: it was respectively 3.3 day of concrete curing for slabs with thickness 2 m and 1.7 day for slabs with thickness 1m. The maximum temperature differences between the center and top surface of the analyzed slabs are observed about 2 days later than the maximum temperature in center has appeared. It is also worth to notice that the development and values of temperatures on the top surface of slabs with different thickness are similar. Additionally, the slabs with thickness 1 m were cooled to the ambient temperature after 20 days.

The results of moisture development are shown in Figure 2b, Figure 2d, Figure 2f, Figure 3c and Figure 3d. The moisture development in the center and on the side surface of the analyzed slabs has the same character and the same amount of moisture was lost during the curing. The differences are observed on the top surface of the slab, where the highest loss of moisture is noticed for the slab with thickness d = 1 m.

Next step of analysis was connected with determination of stress state and cracking area in the analyzed

Table 1.
Thermal and moisture coefficients

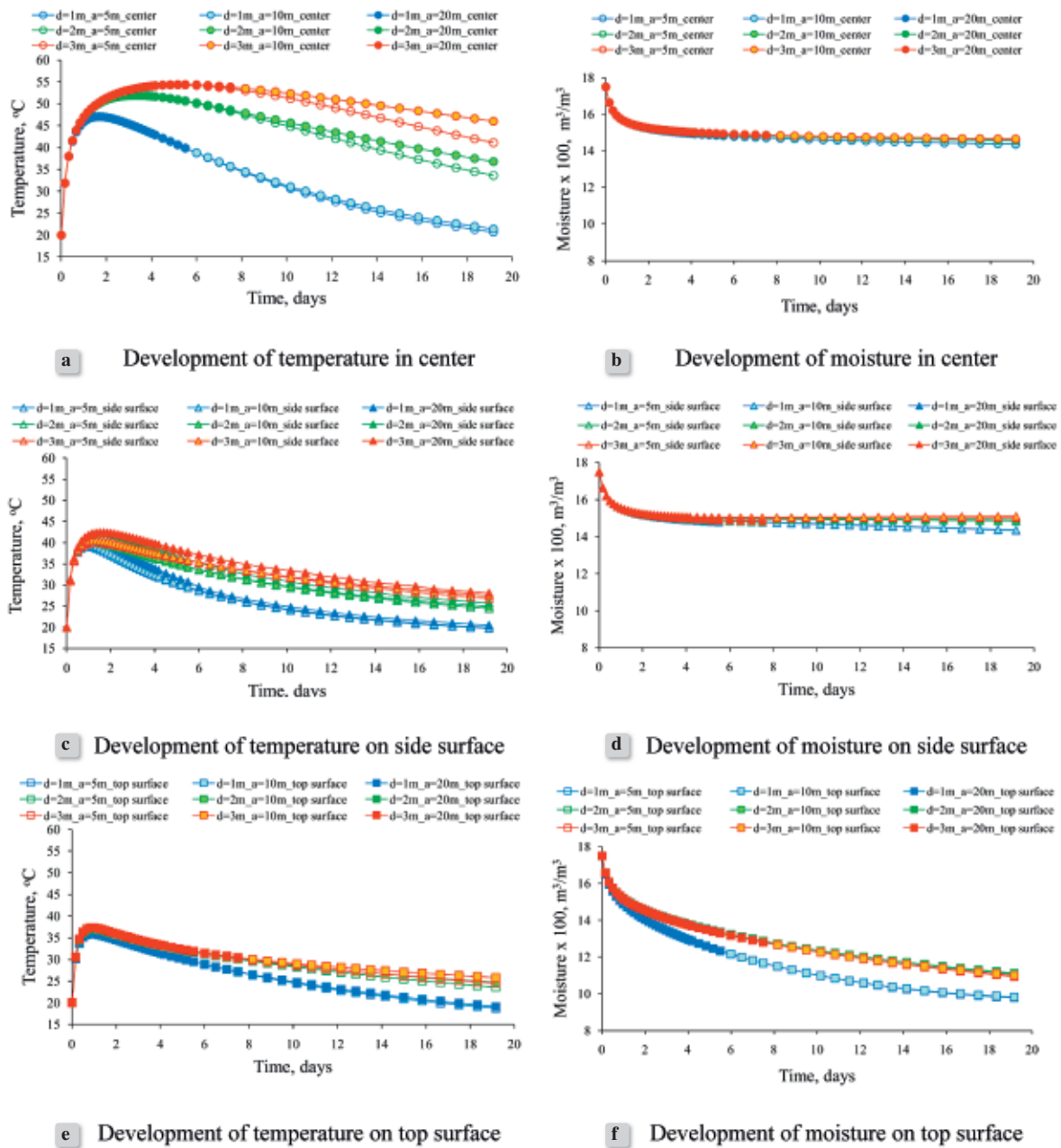| Thermal Fields, Moisture fields			
λ, W/mK	1.75	Heat of hydration	acc. to equation: $Q(T,t) = Q_\infty \, e^{[-at_e^{-0.5}]}$ Q_∞ = 350 kg/kJ, a = 200
c_b, kJ/kgK	1.0		
ρ, kg/m^3	2340	K, m^3/J	0.3 10^{-9}
α_{TT}, m^2/s	7.47 10^{-7}	α_{WW}, m^2/s	0.6 10^{-9}
α_{TW}, m^{2}K/s	9.375 • 10^{-5}	α_{TW}, m^2/sK	2 10^{-11}
α_p, W/m^{2}K	6.00 (without protection) 3.58 (plywood) 0.81 (plywood+soil)	β_p, m/s	2.78 10^{-8} (without protection) 0.18 10^{-8} (plywood) 0.12 10^{-8} (plywood+soil)

Figure 2.
Temperature and moisture development in time for the massive foundation slab with different dimensions

slabs. Figure 4 presents development of stress in time for the massive foundation slab with different dimensions. Two points of the slabs are especially considered: the point in the center of the slab and the central point on the top surface (see Fig. 1). The considered slabs are the example of internally restrained elements where the self-induced stresses are of the great importance. These stresses are related to internal restraints of the structure, resulting from nonuniform volume change in a cross-section. In such elements, during the phase of temperature increase tensile stresses originate in surface layers of the element and compressive stresses are observed inside the element. An inversion of the stress body occurs during
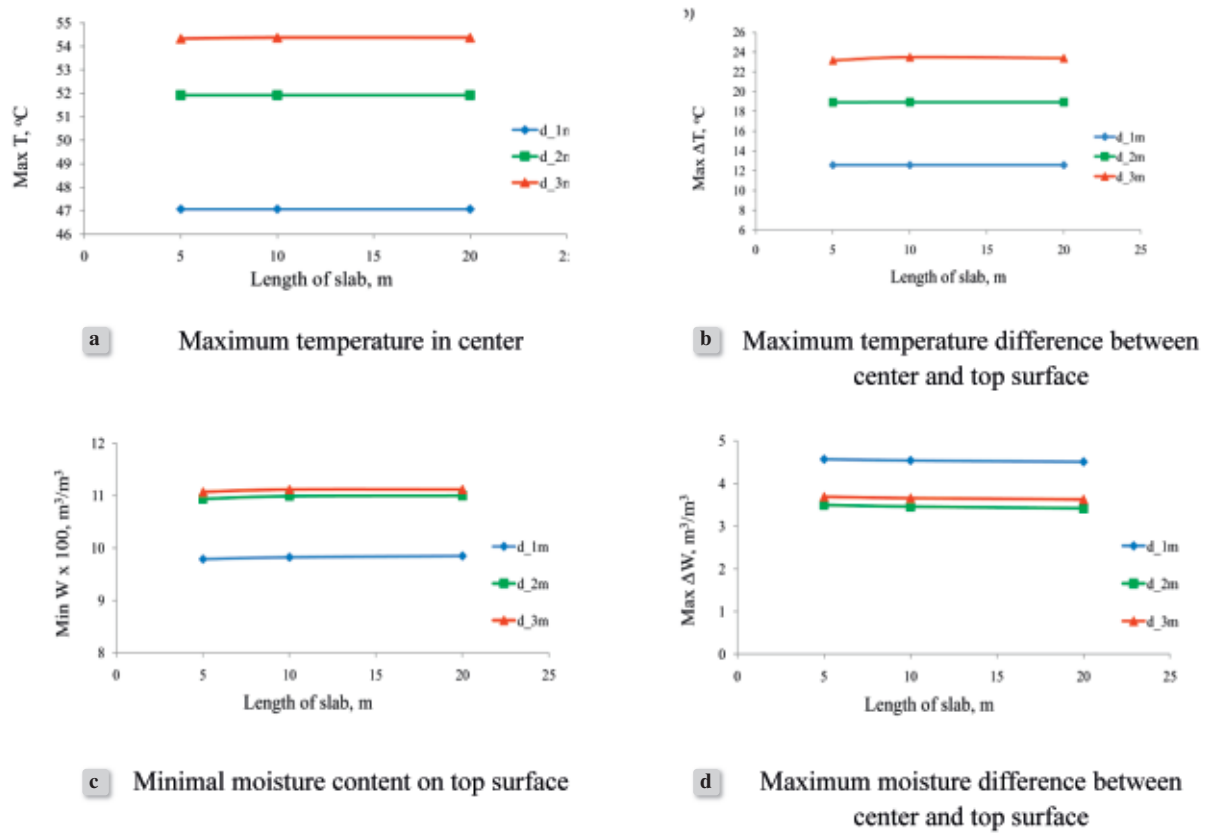
Figure 3.
Comparison of results of thermal and moisture analysis for slabs with different dimensions
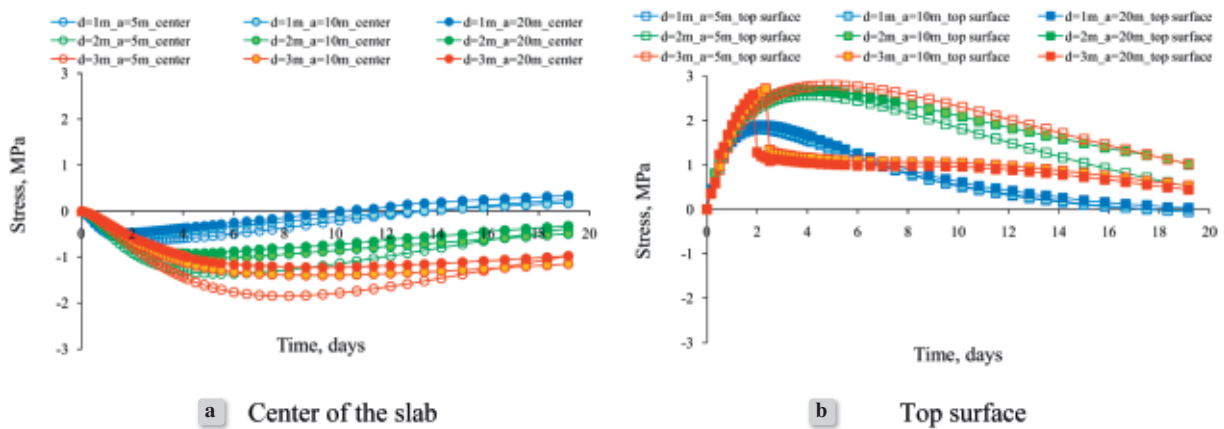

Figure 4.
Development of stress in time for the massive foundation slab with different dimensions

the cooling phase: inside we observe tensile stresses, in the surface layers – compressive stresses. In the analyzed slabs the described inversion of stresses is visible only for the slabs with thickness 1m. In case of greater thickness (2 m or 3 m) the inversion of stresses occurs later.

Table 2.
Description of cracking in analyzed slabs

DIMENSIONS OF SLABS	DESCRIPTION OF CRACKING			
	CENTER AREA	SIDE SURFACE AREA	TOP SURFACE AREA	EDGE AREA
d=1m_a=5m	NO CRACKING	NO CRACKING	NO CRACKING	NO CRACKING
d=2m_a=5m				YES – small area at edge, first cracks in 56 hour after concreting
d=3m_a=5m				YES – small area at edge, first cracks in 52 hour after concreting
d=1m_a=10m			NO CRACKING	NO CRACKING
d=2m_a=10m			NO CRACKING	YES – small area at edge, first cracks in 52 hour after concreting
d=3m_a=10m			YES- first cracks in 52 hour after concreting	YES- small area at edge, first cracks in 44 hour after concreting
d=1m_a=20m			NO CRACKING	NO CRACKING
d=2m_a=20m			NO CRACKING	YES – small area at edge, first cracks in 60 hour after concreting
d=3m_a=20m			YES- first cracks in 44 hour after concreting	YES – small area at edge, first cracks in 40 hour after concreting

a slab d=2m_a=10m   b slab d=3m_a=10m

Figure 5.
Cracking area (black color) on the top surface in analyzed slabs

Rapid decrease of stresses that is visible in Figure 4b for slabs with thickness 3m and base dimensions 10m and 20 m is connected with cracking of the central part of top surface. It is interesting that the first cracks in these two slabs occurred after about 2 days of concrete curing while the maximum temperature in center was observed after 5 days. The time of
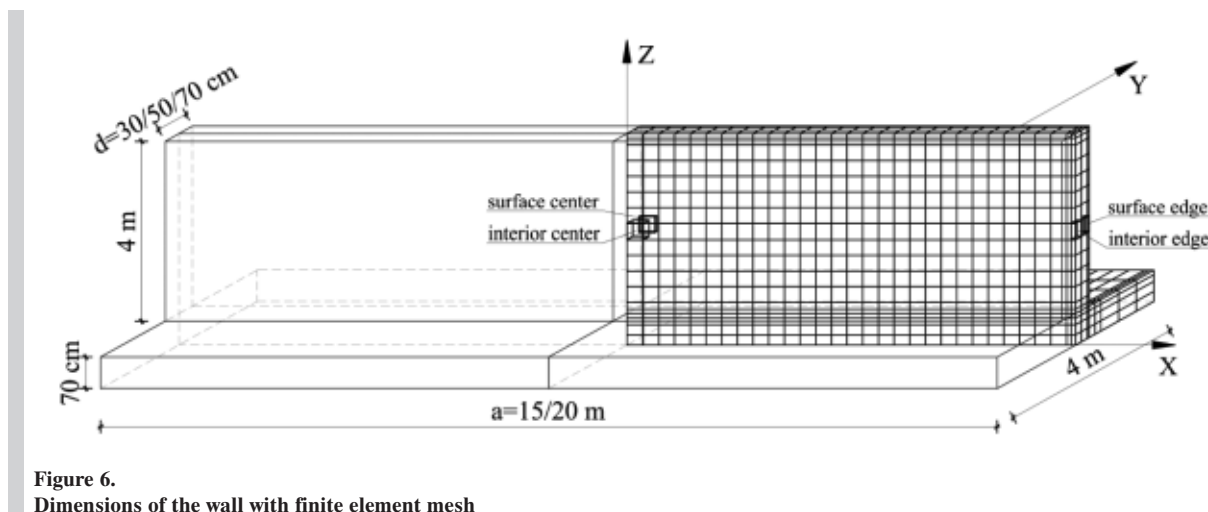
Figure 6.
Dimensions of the wall with finite element mesh

appearance of first cracks is related to the maximum temperature difference between center and top surface equal to 16°C. The detailed description of cracking areas for all slabs is presented in Table 2. Figure 5 presents typical cracking area in the analyzed slabs.

3. MEDIUM-THICK STRUCTURES – RC WALLS

The analysis was also performed for the wall cast against an old set foundation as an example of a medium-thick, externally restrained structure. Similarly, the influence of geometry on the thermal-moisture-mechanical properties was examined. The wall of the 4-m height was analyzed for the length of either 15 or 20 m and three thicknesses: 30, 50 and 70 cm. Six examples being the combinations of these cases were considered. The analyzed wall was supported on a 4-m wide and 70-cm deep strip foundation of the same length. The wall and the foundation were assumed to be reinforced with a near-surface reinforcing net of φ 16 bars. The wall was reinforced at both surfaces with horizontal spacing of 20 cm and vertical spacing of 15 cm. The foundation was reinforced with a 20 cm x 20 cm mesh at the top and bottom surface.

Thanks to a double symmetry of the wall, the model for finite element analysis was created for 1/4 of the wall. A uniform mesh was prepared, densified at free edges of the wall and within the contact surface between the wall and the foundation. Final geometry of the wall with a mesh of finite elements for one exemplary model is presented in Figure 6.

Concrete class C25/30 and steel class RB400 were assumed for both the wall and the foundation. The

foundation was erected earlier and had hardened, so the material properties were assumed as for 28-day concrete, i.e. the compressive strength f_{cm} = 33 MPa, the tensile strength f_{ctm} = 2.6 MPa and the modulus of elasticity E_{cm} = 31 GPa. For the wall, the same final values of the material properties were taken and their development in time was assumed according to CEB-FIP MC90. Detailed material properties, environmental and technological conditions were taken as: cement type CEM I 32.5R, 450 kg/m³, ambient temperature 20°C, initial temperature of fresh concrete mixture 20°C, wooden formwork of 1.8 mm plywood; no insulation; no protection of top surface, formwork removed in 28 days after concrete casting. The foundation was assumed to have cooled down by the moment of the wall casting, thus the initial temperature of the foundation concrete was taken as equal to the ambient temperature. Thermal and moisture coefficients necessary for calculations were taken as for the massive foundation slabs (Table 1), except the heat of hydration, where Q_∞ =420 kg/kJ and a=170 because of a different type of cement assumed.

The thermal-moisture phenomena were analyzed for the first 20 days (480h) after casting of fresh concrete, in time steps. The results for four finite elements were analyzed and compared: in the middle of the wall and on its edge for both internal and surface parts. The chosen elements are presented in Figure 6. Firstly, the thermal effects were considered. The temperature development in time, connected with hydration heat development, was analyzed, and so was the maximum temperature reached in each area of the wall. Figure 7 presents juxtaposition of temperature development diagrams for four areas in the walls with
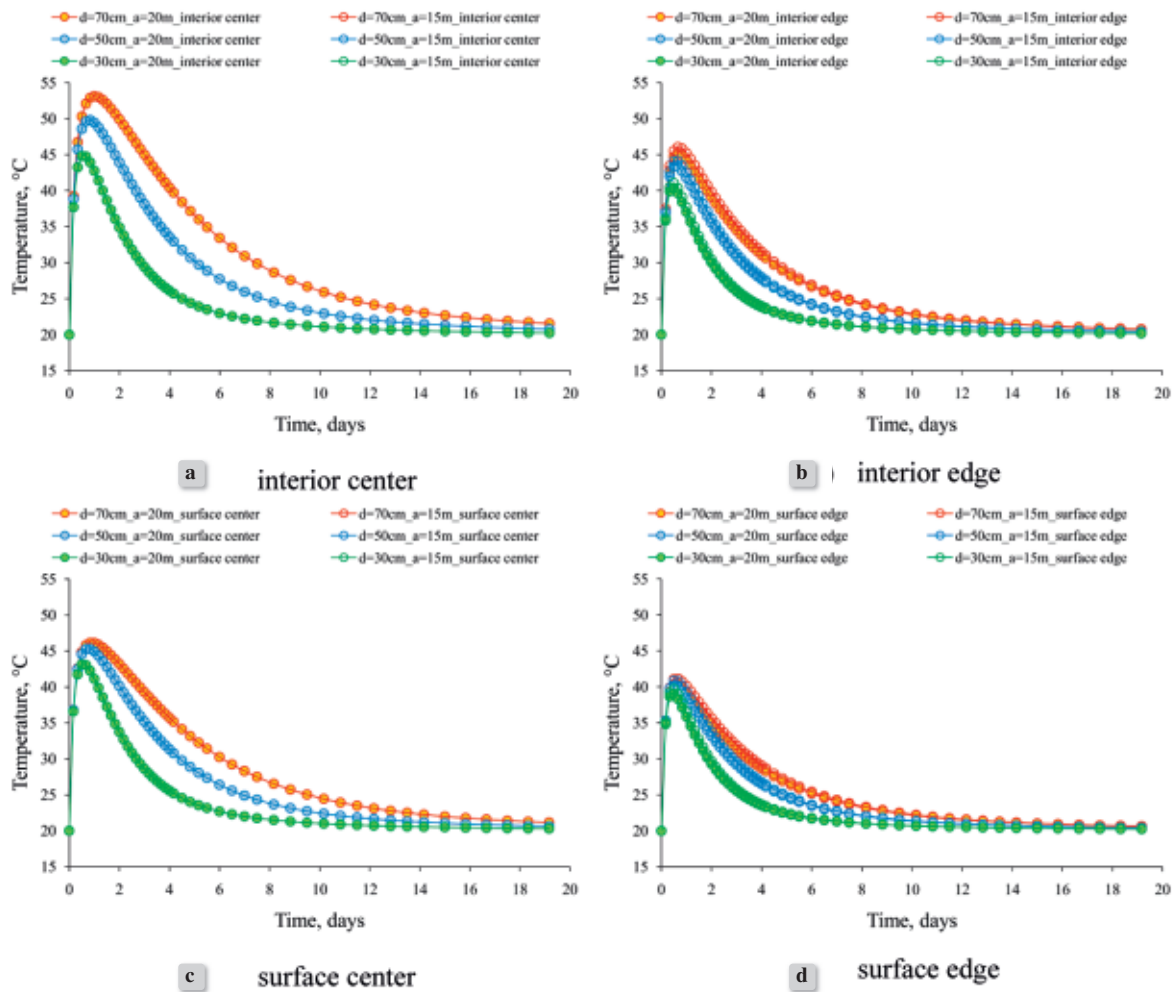
Figure 7.
Temperature development in time for RC walls with different dimensions

different dimensions.

The character of temperature development does not depend on the dimensions of the wall, but the values of the temperatures do. It is visible that the thickness of the wall has the main influence on the temperature development. The greatest temperatures are reached in the thickest walls, which can be noticed especially in the internal part of the wall. The extreme values are reached later in thicker walls; these also cool down more slowly. These phenomena are connected with the ability of heat dissipation which is obviously greater in the thinner walls. There is hardly any influence of the length of the wall on the temperature distribution, at least considering the analyzed cases. No difference is observed in the central part of the wall. Closer to the

free edge of the wall the influence becomes visible, but is of a very small value (less than 1°C).

Then, the moisture effects were considered. The moisture content distribution in time, connected with moisture migration from the wall, as well as the minimum moisture content observed in each area of the wall were analyzed. Figure 8 presents juxtaposition of moisture content development diagrams for four areas in the wall.

The character of the moisture content development is also independent of the geometry of the wall. The observation is very similar as in case of the thermal effects: moisture content distribution depends primarily on the thickness of the wall and not so much on its length. As it can be expected, water migration
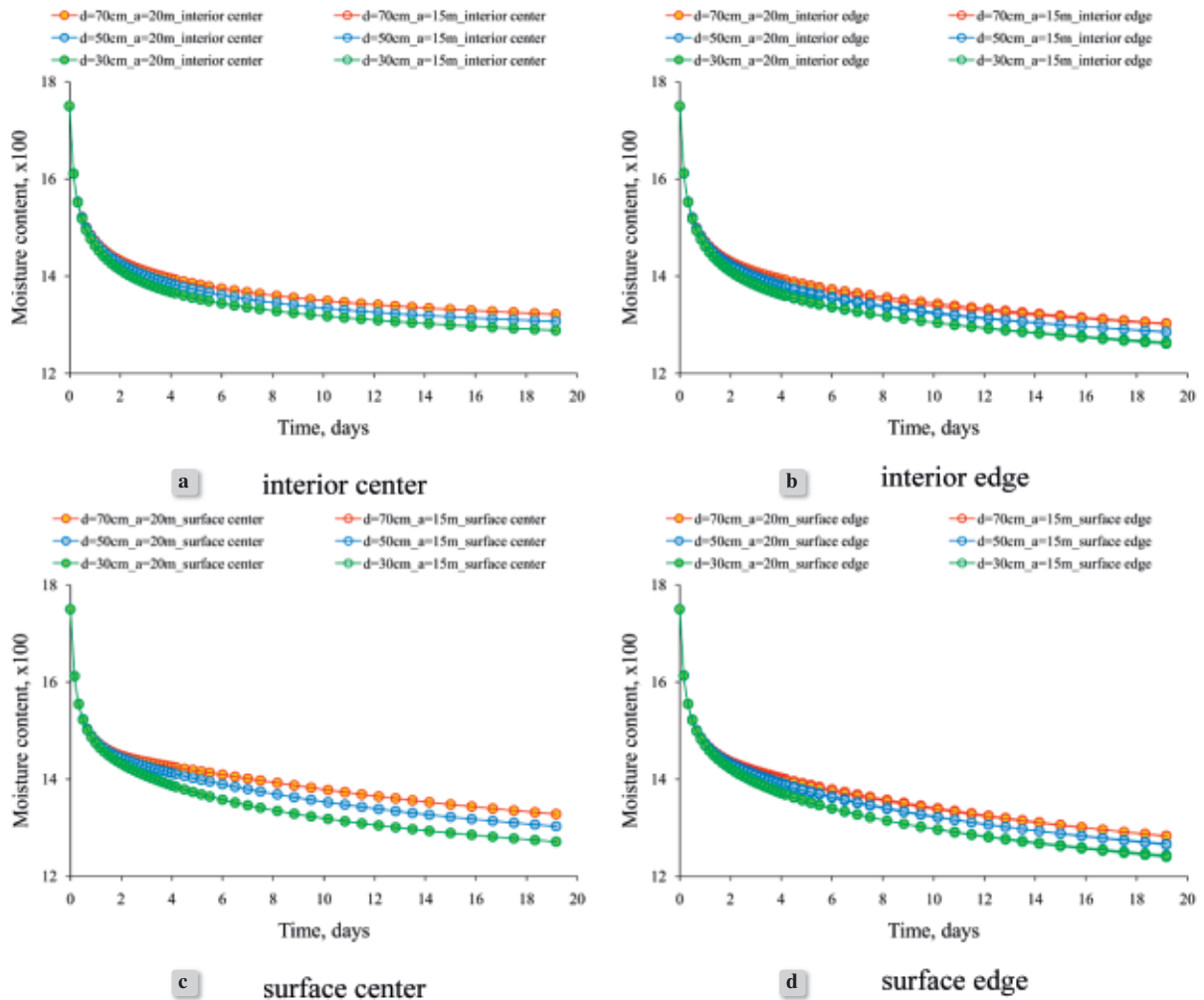
Figure 8.

Moisture content development in time for RC walls with different dimensions m^3/m^3

from the wall is the fastest and the most intensive in the thinnest walls. The influence of the wall length is even smaller in case of the moisture effects than in case of the thermal effects. No difference is observed in the central part of the wall. Closer to the free edge of the wall the influence becomes visible, but vanishes as the wall gets thicker.

Figure 9a shows the comparison of maximum temperatures reached for different dimensions of the wall on the example of internal part in the midspan of the wall while Figure 9b presents the maximum temperature difference between the interior and the surface of the wall in its central part in all the analyzed cases. Figure 9c shows the comparison of minimum moisture contents reached for different dimensions of the wall on the example of internal part in the

midspan of the wall while Figure 9d presents the maximum moisture content difference between the interior and the surface of the wall in its central part in all the analyzed cases.

Determination of the thermal-moisture fields allowed to indicate the stress state in the wall. Stress development in time was analyzed for one part of the wall, i.e. the interior of the wall in its central part, where the concentration of stresses is observed. The obtained results were collectively presented on a diagram in Figure 10. Rapid decrease of stresses that is visible in Figure 10 for walls with length 20m is connected with cracking of the point described as a interior center (see Fig. 6).
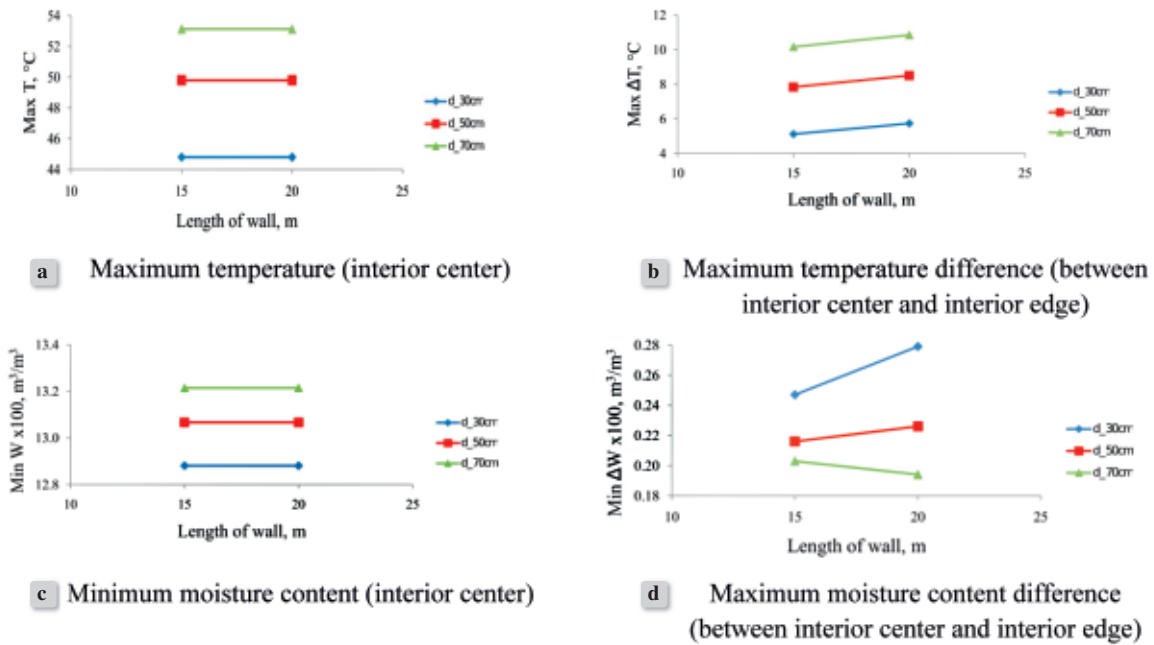
a — Maximum temperature (interior center)

b — Maximum temperature difference (between interior center and interior edge)

c — Minimum moisture content (interior center)

d — Maximum moisture content difference (between interior center and interior edge)

Figure 9.
Comparison of results of thermal and moisture analysis for walls with different dimensions
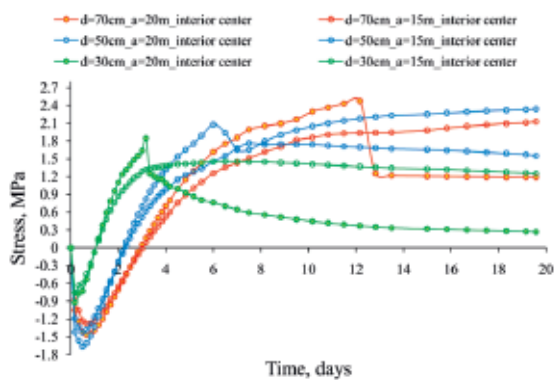

Figure 10.
Stress development in time (interior center)

A typical two-phase (compressive-tensile) character of stress development in time is observed in each analyzed case. In the first phase concrete temperature increases (self-heating) and the wall extends being opposed by the weakly bonded foundation, which results in occurrence of compressive stresses (Fig. 11a). In the second phase the wall starts to cool down, restrained by a cooled foundation, which leads to development of tensile stresses in the wall (Fig. 11b).

As far as the stresses are concerned, both the thickness and the length of the wall have an influence on their distribution and values. Comparing stress distribution in the walls of the same length but various thicknesses it can be noted that lower values of compressive stresses are reached in thinner walls, an so the stress inversion is faster and tensile stresses occur earlier. These stresses can reach significant values which may lead to cracking. It also has to be emphasized that tensile strength of concrete at such an early age (about 2 days) is very low, which additionally contributes to undesired cracking. In thicker walls (50 cm, 70 cm) the inversion occurs later, so tensile stresses can reach greater values without posing a risk of cracking. If cracking is caused, it occurs later: for the analyzed walls it is 6 and 12 days for 50 cm and 70 cm thick wall, respectively.

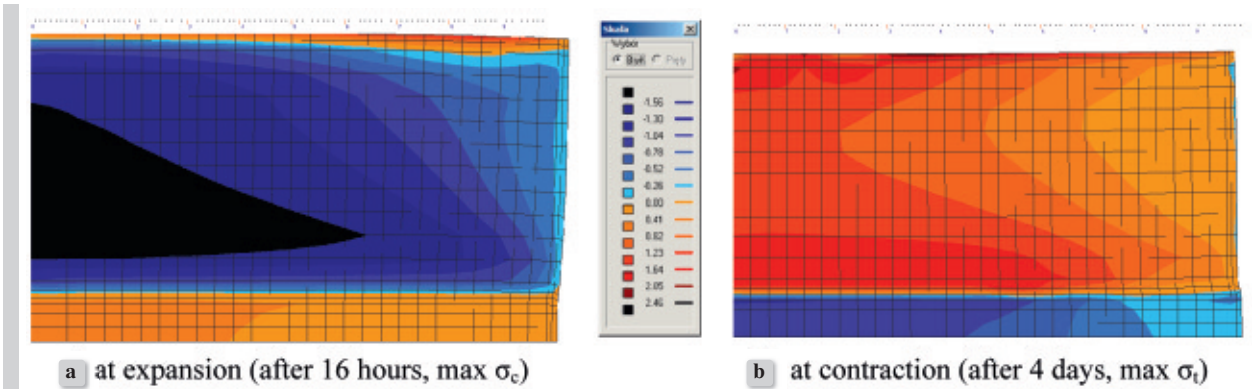Analyzing the walls of the same thickness but various

a at expansion (after 16 hours, max σ_c)

b at contraction (after 4 days, max σ_t)

Figure 11.
Exemplary maps of stress distribution (d_50cm, a_20m), XZ = 0 m

Table 3.
Description of cracking pattern in the walls

DIMENSIONS OF WALLS	DESCRIPTION OF CRACKING
d_70cm, a_20m	First cracks occur after ~3.5 days at the connection between the wall and the foundation, near the free edge of the wall and – in time – advance towards the central part of the wall. Severe cracking observed in the central part of the wall; cracking intensity diminishes towards the free edge. Cracks develop towards the interior of the wall – little cracking observed on the surface.
d_50cm, a_20m	First cracks occur after ~3 days at the connection between the wall and the foundation, near the free edge of the wall and – in time – advance towards the central part of the wall. Intensive cracking observed in the central part of the wall; cracking intensity diminishes towards the free edge. Cracks develop towards the interior of the wall, nevertheless, significant cracking is observed on the surface.
d_30cm, a_20m	First cracks occur after ~1.5 days at the connection between the wall and the foundation, near the free edge of the wall and – in time – advance towards the central part of the wall. Cracks of considerable intensity concentrate in the central part of the wall. Cracks develop towards the interior of the wall. Comparable intensity of cracking is observed in the internal and surface part of the wall.
d_70cm, a_15m	First cracks occur after ~3 days at the connection between the wall and the foundation, near the free edge of the wall and – in time – advance towards the central part of the wall. Higher cracking is observed in the central part of the wall; cracking intensity diminishes towards the free edge. Cracks develop towards the interior of the wall – little cracking observed on the surface.
d_50cm, a_15m	Small cracks occur after ~2.5 days at the connection between the wall and the foundation, near the free edge of the wall. Cracks develop towards the interior of the wall – hardly any cracking observed on the surface.
d_30cm, a_15m	Small cracks occur after ~1.5 days at the connection between the wall and the foundation, near the free edge of the wall. and – in time – advance towards the central part of the wall. Cracks develop towards the interior of the wall - hardly any cracking observed on the surface.

lengths it can be observed that greater values of stresses – both compressive and tensile – are reached and cracking risk is greater in the longer walls despite very similar values of thermal and moisture effects. It is connected with greater linear resistance caused by foundation restraint. In the cases considered no cracking was observed in 15-m long wall. Table 3 presents a detailed description and comparison of cracking areas and cracking development in time for all analyzed cases. Figures 12-13 show final cracking area (filled with black colour) in the interior and on the surface of the walls.

It can be summarized that the character of cracking pattern does not depend on the dimensions of the wall, while cracking intensity and development rate complies with the observed stress development and depends primarily on the length of the wall. In all cases cracking was initiated at the wall-foundation interface in the vicinity of the free edge and proceeded towards the central part of the wall, where concentration of cracking was observed in the end of the hardening process. As the wall was assumed to be kept in formwork for the
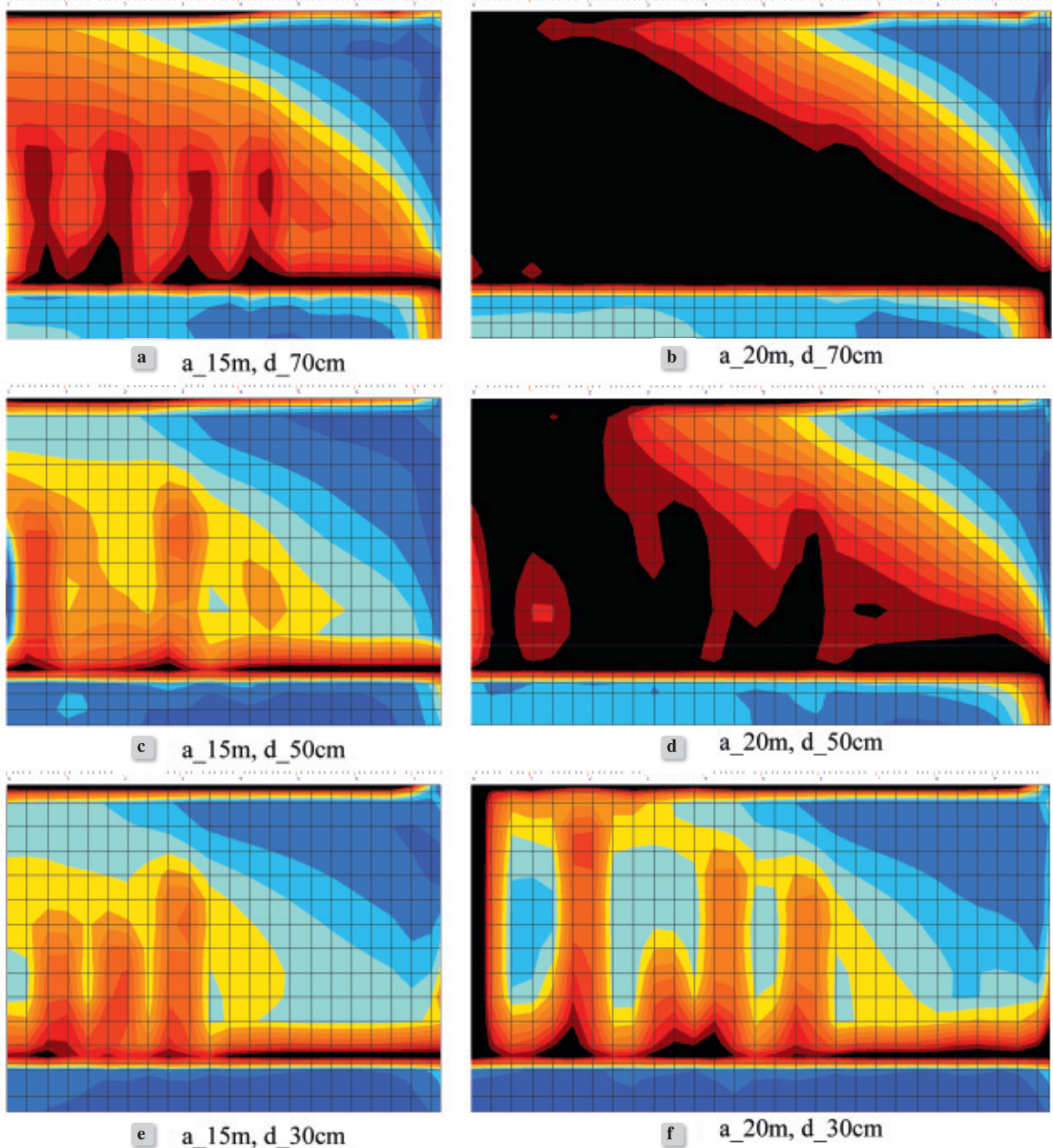
Figure 12.
Final cracking pattern (cracked areas in black), interior of the walls

whole cooling process, cracking development towards the interior of the wall was observed, too.

Cracking of significantly greater intensity was observed in longer walls: severe cracking occurred in 20-m long walls, especially the thick ones, while almost no cracking occurred in the 15-m long walls. The thickness of the wall had minor influence on the

cracking intensity, but it influenced the cracking rate (thicker walls cracked later) and cracking distribution within the cross section (smaller differences in cracking pattern between the interior and the surface were observed in thinner walls).
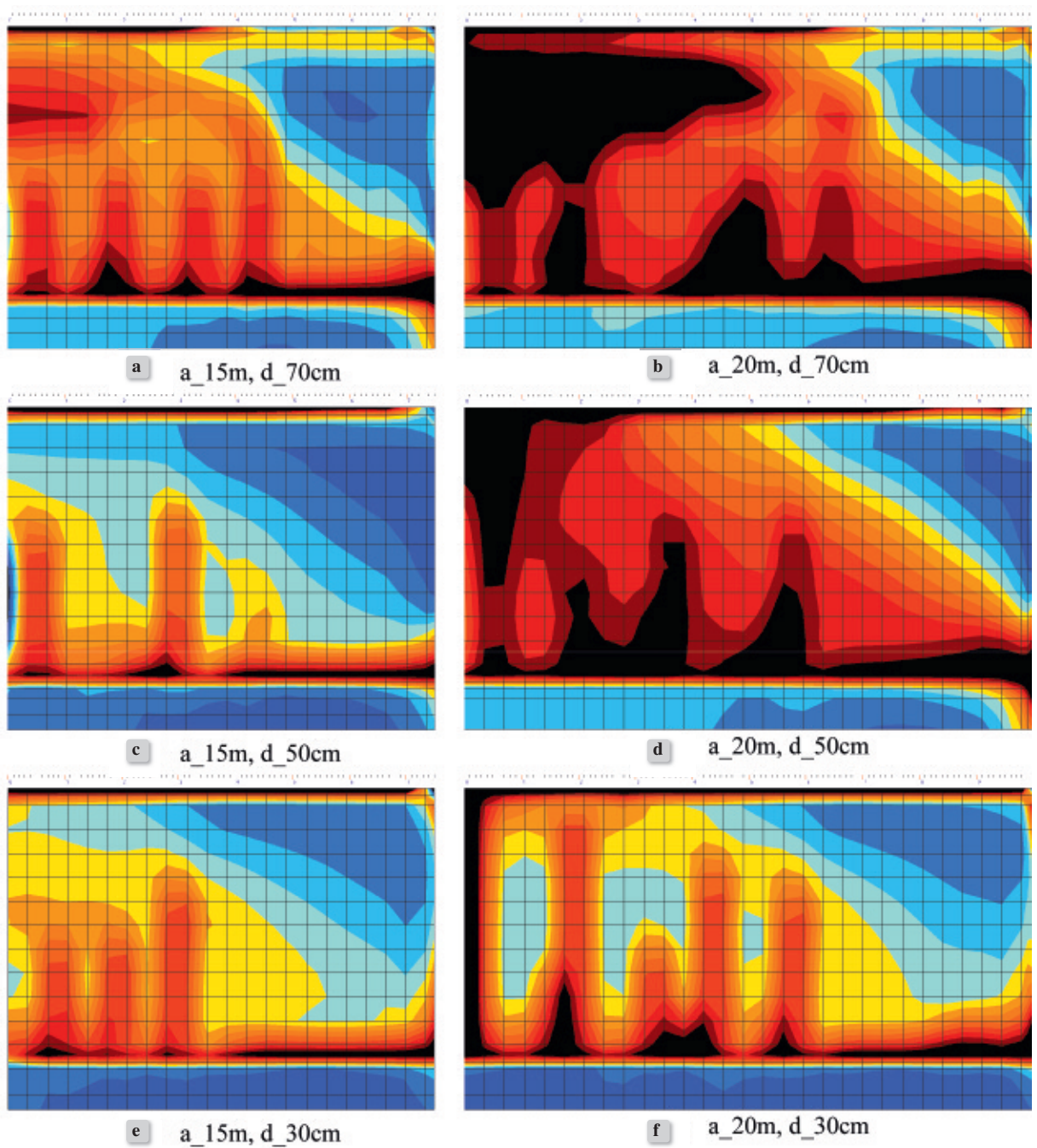
a   a_15m, d_70cm

b   a_20m, d_70cm

c   a_15m, d_50cm

d   a_20m, d_50cm

e   a_15m, d_30cm

f   a_20m, d_30cm

Figure 13.
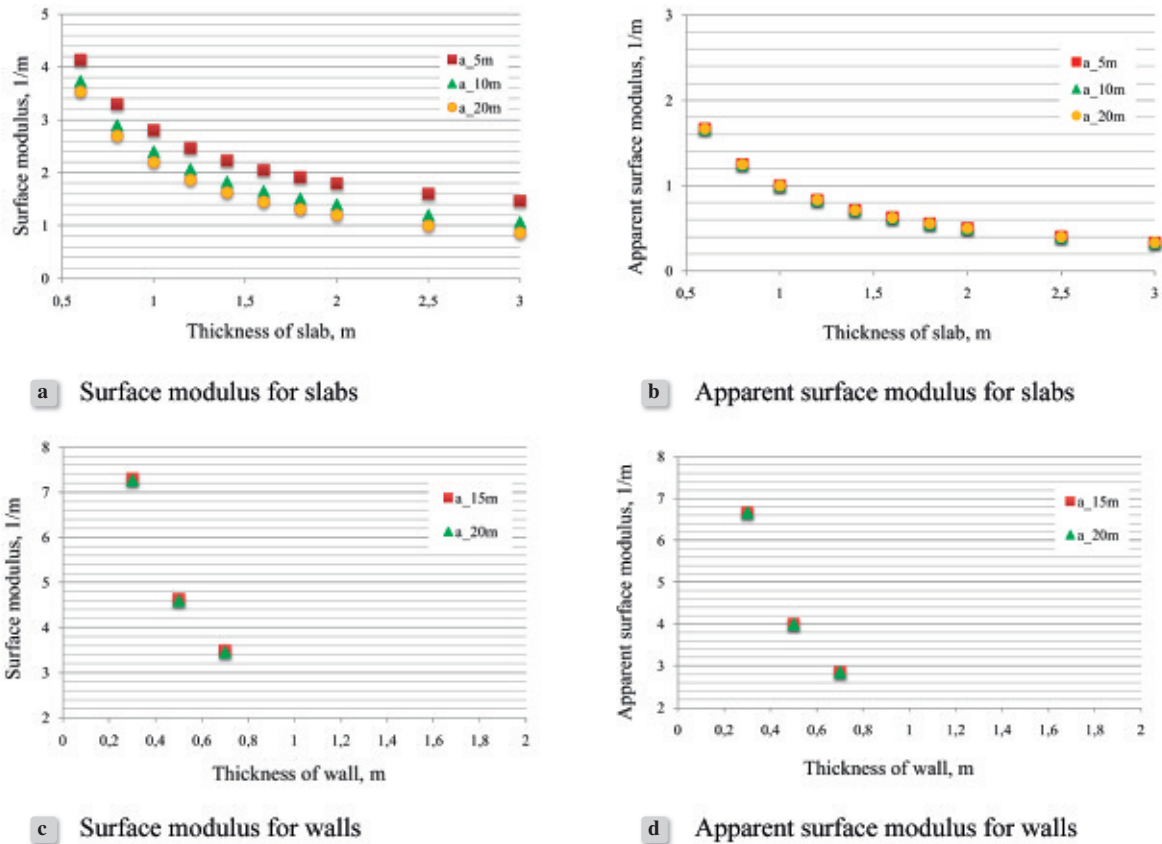**Final cracking pattern (cracked areas in black), surface of the walls**

Figure 14.
Surface and apparent modulus for analyzed slabs and walls

4. TESTS RESULTS RELATED TO MEAUSURES OF THERMAL-SHRINKAGE SENSITIVITY

As it was mentioned in the Introduction, to assess the sensitivity of structures to early age thermal and shrinkage effects as well as the cracking risk some measures are proposed. These measures are the surface modulus, the apparent surface modulus as well as the equivalent thickness. Figures 14 presents the considered dimensions of slabs and walls related to the values of the surface modulus and to the apparent modulus. The apparent modulus for slabs was calculated by taking the area S_p as the area of top surface which is cooled more intensively than others. For walls the area S_p was taken as the area of longitudinal vertical surfaces, which are the mainly cooled surfaces. Because the equivalent thickness is the inverse of the apparent surface modulus ($d_e = 1/m_p$) the relation between the dimensions and the equivalent thickness is similar to the relation obtained for the

apparent surface modulus. Taking into account the classification of structures related to the surface modulus slabs with thickness d=2m and d=3m should be considered as massive elements. The slabs with thickness d=1m can be treated as medium-thick structures. The surface modulus for walls is greater than the limit value m=2, therefore the analyzed walls can be classified as the medium-thick elements. It can also be noticed from Figure 14 that the value of the apparent modulus for slabs does not depend on the base dimensions of the slabs and it is only the function of thickness. In case of walls both the surface and apparent modulus depend only on the thickness of the wall (for the same height of the wall).

Next, the thermal analysis results were compared in relation to the values of surface modulus and the values of equivalent thickness. Figure 15 presents the maximum temperatures generated during the hydration process related to the above measures. It can be seen from Figure 15a that some slabs have similar value of surface modulus but the maximum tempera-
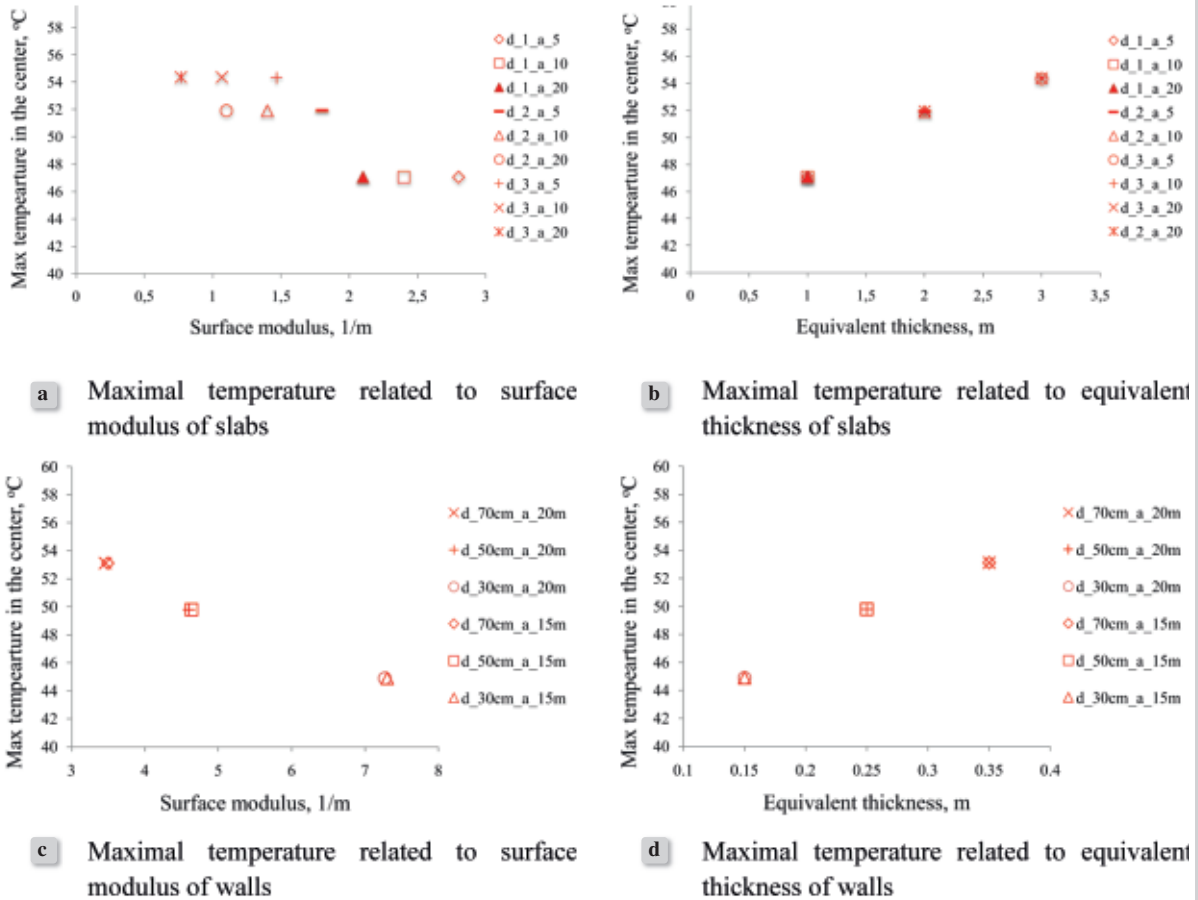
Figure 15.
Maximal temperature in slabs and walls related to their surface modulus and equivalent thickness

tures are different. It is visible, for example, when the slab d_2_a_10 (with thickness 2m and dimensions of base 20×20m – the surface modulus is equal to 1.4) where the maximum temperature is equal to 51.9°C is compared to the slab d_3_a_5 (the surface modulus is equal to 1.47) where the maximum temperature is equal to 54.3°C. The same applies to the maximum temperature differences between the center and top surface of the slabs. For slab d_2_a_10 value 18.9°C is obtained while for slab d_3_a_5 it is 23.2°C, but it should be emphasized that these values are close to the suggested value of 20°C for elements with surface modulus lower than 2.

There are not such disagreements when the results are related to the equivalent thickness, which is perfectly visible in Figure 15b. What is interesting in case of walls there are no discussed differences in comparison of tests results to the surface modulus and equivalent thickness (see Fig. 15c and Fig.15d).

The cracking sensitivity can be also related to the discussed measures and some proposals from literature suggest that elements are sensitive to early age thermal effects when $m<2$. For the slabs with the surface modulus greater than 2 (slabs with thickness 1m) no cracks are observed – it is in agreement with above suggestions. The cracks were observed in slabs with and the largest cracking area is visible for slabs with the surface modulus equal to 1.1 (d_3_a_10) and 0.8 (d_3_a_20) – see Table 2 and Figure 5.

It should be also added that for the externally restrained elements such as RC walls the above mentioned measure of cracking sensitivity is not suitable. All analyzed walls are classified as medium-thick structures with $m \geq 2$ while large cracking areas were noted (see Fig. 12 and Fig. 13).

5. CONCLUSIONS

Control of thermal and shrinkage cracking in early age concrete is of great importance to ensure a desired service life and function of structures. It is a complicated problem due to complex nature of interacting phenomena and large number of contributing factors [7, 8, 9, 10]. One of the important factors is the geometry and the dimensions of structural elements as well as kind of restraint. This paper discusses the influence of the type and dimensions of a structure on the distribution of temperature, moisture and induced stresses. Two kinds of restraint – external and internal – are also investigated here. Two types of structures were selected for the analysis: the massive foundation slab as the example of internally restraint structure and the reinforced concrete wall as the example of externally restraint structure. It should be pointed that presented results are related to the assumed, simplified curing conditions as constant ambient temperature and constant air humidity. In practical prediction of the cracking risk in concrete structures the assumed environmental conditions should consider the real temperatures and humidity over the analyzed period.

The proposed measures for early age cracking sensitivity are also discussed in the paper in relation to the obtained results. The conducted comparative analysis indicates that the equivalent thickness can be considered as proper measure when the cooling conditions are different for the top and the rest of surfaces of the element. It should be also noticed that elements classified as medium-thick structures can be also sensitive to early age cracking of thermal and shrinkage origin.

ACKNOWLEDGEMENT

REFERENCES

[1] ACI Committee No 207.2R; Effect of Restraint, Volume Change, and Reinforcement on Cracking of Mass Concrete, ACI Materials Journal, Vol.87, No.3, 1990; p.271-295

[2] *Flaga K.*; Naprężenia własne termiczne typu "makro" w elementach i konstrukcjach z betonu (Macro self-induced thermal stresses in concrete elements and structures), Monography 106 of Cracow Technical University, 1990 (in Polish)

[3] *Flaga K.*; Naprężenia skurczowe i zbrojenie przypowierzchniowe w konstrukcjach betonowych (Shrinkage stresses and surface reinforcement in concrete structures). Monography of Cracow Technical University, 2011 (in Polish)

[4] *Kiernożycki W.*; Betonowe konstrukcje masywne (Massive concrete structures). Polski Cement, Kraków 2003 (in Polish)

[5] *De Schutter G., Taerwe L.*; Estimation of Early-Age Thermal Cracking Tendency of Massive Concrete Elements By Means of Equivalent Thickness. ACI Materials Journal, Vol.93, No.5, 1996; p.403-408

[6] *Witakowski P.*; Technologia budowy konstrukcji masywnych z betonu (Technology of Massive Concrete Structures), XIII Konferencja Naukowa – Korbielów 2001 "Metody Komputerowe w Projektowaniu i Analizie Konstrukcji Hydrotechnicznych" (in Polish)

[7] *Klemczak B., Knoppik-Wróbel A.*; Early age thermal and shrinkage cracks in concrete structures – description of the problem, Architecture-Civil Engineering-Environment, Vol.4, No.2, 2011; p.35-48.

[8] *Klemczak B.*; Modelowanie efektów termiczno-wilgotnościowych i mechanicznych w betonowych konstrukcjach masywnych (Modelling the thermal-moisture and mechanical effects in massive concrete structures). Monografia 183, Wydawnictwo Politechniki Śląskiej, Gliwice 2008 (in Polish)

[9] *Klemczak B.*; Prediction of Coupled Heat and Moisture Transfer in Early-Age Massive Concrete Structures. Numerical Heat Transfer. Part A: Applications, Vol.60, No.3, 2011; p.212-233

[10] Thermal Cracking in Concrete at Early Ages. Proceedings of the International Rilem Symposium, Chapman &Hall, London, 1994